

Effects of macroscopic polarization in III-V nitride multi-quantum-wells

Vincenzo Fiorentini

*Istituto Nazionale per la Fisica della Materia – Dipartimento di Fisica, Università di Cagliari, Cagliari, Italy, and
Walter Schottky Institut, Technische Universität München, Garching, Germany*

Fabio Bernardini

Istituto Nazionale per la Fisica della Materia – Dipartimento di Fisica, Università di Cagliari, Cagliari, Italy

Fabio Della Sala, Aldo Di Carlo, and Paolo Lugli

*Istituto Nazionale per la Fisica della Materia – Dipartimento di Ingegneria Elettronica, Università di Roma “Tor Vergata”,
Roma, Italy*

(resub to PRB 28 dec 99)

Huge built-in electric fields have been predicted to exist in wurtzite III-V nitrides thin films and multilayers. Such fields originate from heterointerface discontinuities of the macroscopic bulk polarization of the nitrides. Here we discuss the background theory, the role of spontaneous polarization in this context, and the practical implications of built-in polarization fields in nitride nanostructures. To support our arguments, we present detailed self-consistent tight-binding simulations of typical nitride QW structures in which polarization effects are dominant.

73.40.Kp, 77.22.Ej, 73.20.Dx

I. INTRODUCTION

Spontaneous polarization has long been known to take place in ferroelectrics. On the other hand, its existence in semiconductors with sufficiently low crystal symmetry (wurtzite, at the very least) has been generally regarded as of purely theoretical interest. Recently, a series of first principles calculations^{1–3} has reopened this issue for the technologically relevant III-V nitride semiconductors, whose natural crystal structure is, in fact, wurtzite. Firstly,¹ it was shown that the nitrides have a very large spontaneous polarization, as well as large piezoelectric coupling constants. Secondly,^{2,3} it was directly demonstrated how polarization actually manifests itself as electrostatic fields in nitride multilayers, due to the polarization charges resulting from polarization discontinuities at heterointerfaces. This charge-polarization relation, counterchecked in actual *ab initio* calculations,³ has been exploited to calculate dielectric constants.²

While piezoelectricity-related properties are largely standard, spontaneous polarization is to some extent new in semiconductor physics, to the point that, so far, the practical importance of spontaneous polarization in III-V nitrides nanostructures (multi quantum wells, or MQWs, are the focus of this paper) has been largely overlooked. It is tantalizingly clear to us, however, that these concepts may lead to a direct and unambiguous measurement of the spontaneous polarization in semiconductors, to the recognition of its importance in nitride-based nanostructures, and, hopefully, to its exploitation in device applications. Our work has already spawned interpretations⁴ and purposely planned experiments⁵ in this direction; in the hope of accelerating the process, in this paper we show how to account for the effects of spontaneous polarization in MQWs, and discuss some

prototypical cases and their possible experimental realization. To support our arguments, we present simulations of typical AlGaIn/GaN MQWs where spontaneous and piezoelectric polarizations are about equal.

Among the consequences of macroscopic polarization which we will demonstrate in this paper let us mention the following: (a) the field caused by the fixed polarization charge, superimposed on the compositional confinement potential of the MQW, red-shifts dramatically the transition energies and strongly suppresses interband transitions as the well thickness increases; (b) the effects of thermal carrier screening are negligible in typical MQWs, although not in massive samples; (c) a quasi-flat-band MQW profile can be approximately recovered (*i.e.* polarization fields can be screened) only in the presence of very high free-carrier densities, appreciably larger than those typical of semiconductor laser structures; (d) even in the latter case, transition probabilities remain considerably smaller than the ideal flat band values, and this reduces quantum efficiency; (e) once an appropriate screening density (*i.e.* the pumping power or injection current) has been chosen to ensure that the recombination rate is sufficient, a residual polarization fields is typically still present: this provides a means to intentionally red-shift transition energies by changing well thicknesses, without changing composition; (f) the very existence of distinct and separately controllable spontaneous and piezoelectric polarization components allows to choose a composition such that they cancel each other out, leading to flat-band conditions. Analogously, for a proper choice of superlattice composition, piezoelectric polarization can be made to vanish and hence a measure of spontaneous polarization can be accessed, through *e.g.* the changes in optical spectra. It is clear that a fuller understanding of these points will ultimately lead both to

improvements in design and operation of real nitride devices, and to the direct measurement of polarization, and a better knowledge thereof, in nitride semiconductors.

Before moving on, let us mention other recent contributions in this area. Buongiorno Nardelli, Rapcewicz, and Bernholc, using non-self-consistent effective-mass based perturbation theory in the small field limit, have predicted⁶ red shifts and transition probability suppression in InGaN quantum well; Della Sala *et al.*, using self-consistent tight binding calculations, have applied⁷ some of the ideas reported in this paper to InGaN/GaN quantum well lasers, explaining several puzzling experimental features, among which the high thresholds observed for GaN-based lasers, and several other aspects related to self-consistent screening effects; Montecarlo simulations⁸ by Oberhuber, Vogl, and Zandler, employing the polarization calculated in Ref. 1, have revealed a polarization-enhanced carrier density in the conduction channel of AlGaIn/GaN HEMTs. Takeuchi *et al.* have interpreted⁹ their own measurement of a quantum-confined Stark effect in InGaIn/GaN superlattices as piezoelectricity-induced; this is, as it turns out, essentially correct in their specific case involving InGaIn, but not in general. Analogous results have been reported in Refs. 10 and 11, the latter including fairly detailed simulations, but only accounting for piezoelectricity. Finally, a detailed theoretical exposition of effective-mass theory adapted to deal with piezoelectric fields is given in Ref. 12, including useful notation and basic formulas, and some applications. Experimental work will be mentioned later; here let us just quote the very recent evidence that polarization-related effects on optical properties in selected AlGaIn/GaN systems cannot be properly interpreted if spontaneous polarization is neglected; circumstantial evidence was obtained⁴ by Leroux *et al.*, while a more carefully planned investigation, reaching firmer conclusions, has been carried out⁵ by Cingolani *et al.*

II. PIEZOELECTRIC FIELDS

Piezoelectricity is a well known concept in semiconductor physics. Binary compounds of strategic technological importance as III-V arsenides and phosphides can be forced to exhibit piezoelectric polarization fields by imposing upon them a strain field.

Among others, applications of piezoelectric effects in semiconductor nanotechnology exist in the area of multi quantum-well (MQW) devices. A thin semiconductor layer (active layer) is embedded in a semiconductor matrix (cladding layers) having a different lattice constant. If pseudomorphic growth occurs, the active layer will be strained and therefore subjected to a piezoelectric polarization field, which can be computed as

$$\mathbf{P}^{(pz)} = \vec{\epsilon} \cdot \vec{\epsilon} \quad (1)$$

if the strain field $\vec{\epsilon}$ and the piezoelectric constants tensor $\vec{\epsilon}$ are known.

In a finite system, the existence of a polarization field implies the presence of electric fields. For the piezoelectric case, the magnitude of the latter depends on strain, piezoelectric constants, and (crucially) on device geometry. The structure of a typical III-V nitride-based superlattice or MQW is $-C-A-C-A-C-A-C-$ (A=active, C=cladding), where both the cladding layer and the active layer are in general strained to comply with the substrate in-plane lattice parameter. In such a structure, the electric fields in the A and C layers are

$$\begin{aligned} \mathbf{E}_A^{(pz)} &= 4\pi\ell_C(\mathbf{P}_C^{(pz)} - \mathbf{P}_A^{(pz)})/(\ell_C\epsilon_A + \ell_A\epsilon_C) \\ \mathbf{E}_C^{(pz)} &= 4\pi\ell_A(\mathbf{P}_A^{(pz)} - \mathbf{P}_C^{(pz)})/(\ell_C\epsilon_A + \ell_A\epsilon_C) \end{aligned} \quad (2)$$

where $\epsilon_{A,C}$ are the dielectric constants and $\ell_{A,C}$ the thicknesses of layers A and C. Thus, in general, an electric field will be present whenever $\mathbf{P}_A \neq \mathbf{P}_C$. The above expressions are easily obtained¹³ by the conditions that the electric displacement be conserved along the growth axis, and by the boundary conditions that the potential energy on the far right and left of the MQW structure are the same.¹⁴

There are essentially three special cases of MQW structures worth mentioning:

- i) active (cladding) layer lattice matched to the substrate: $\mathbf{P}_A = 0$ ($\mathbf{P}_C = 0$);
- ii) $\ell_A = \ell_C$, whence $\mathbf{E}_A = -\mathbf{E}_C$;
- iii) $\ell_A \ll \ell_C$, implying $\mathbf{E}_C \simeq 0$, and hence

$$\mathbf{E}_A^{(pz)} = 4\pi\mathbf{P}_A^{(pz)}/\epsilon_A. \quad (3)$$

In the last case we implicitly assumed the cladding layer to be unstrained – that is, its lattice constant to be relaxed to its equilibrium value because its thickness exceeds the critical value for pseudomorphic growth over the substrate. $\mathbf{P}^{(pz)}$ may take any direction in general, but in normal practice its direction is parallel to the growth axis.¹⁵

To obtain piezoelectric polarization effects in zincblende semiconductor systems, lattice-mismatched epitaxial layers are purposely grown along a polar axis, *e.g.* (111); the in-plane strain propagates elastically onto the growth direction, thereby generating $\mathbf{P}^{(pz)}$. In wurtzite nitrides, the preferred growth direction is the polar (0001) [or (000 $\bar{1}$)] axis, so that any non-accomodated in-plane mismatch automatically generates a piezoelectric polarization along the growth axis (the sign depends on whether the epitaxial strain is compressive or tensile). We will be always be assuming this situation in the following.

Usually, alloys are employed in the fabrication of MQWs. In that case, one may estimate the piezoelectric polarization in the spirit of Vegard's law as, for a general strain imposed upon *e.g.* an $\text{Al}_x\text{Ga}_{1-x}\text{N}$ alloy,

$$\mathbf{P}^{(\text{pz})} = [x \vec{e}_{\text{AlN}} + (1-x) \vec{e}_{\text{GaN}}] \vec{e}(x), \quad (4)$$

This expression contains terms linear as well as quadratic in x , and similar relations hold for quaternary alloys. This piezoelectric term is only present in pseudomorphic strained growth, and will typically tend to zero beyond the critical thickness at which strain relaxation sets in. Uncomfortable though it may be,¹⁶ the Vegard hypothesis is at this point in time the only way to account for piezoelectric (and spontaneous, see below) fields in alloys. As will be shown below, indeed, the qualitative picture does not depend so much on the detailed value of the polarization field as on their order of magnitude.

III. SPONTANEOUS FIELDS IN MQWS

New possibilities are opened by the use of III-V nitrides (AlN, GaN, InN), that naturally crystallize in the wurtzite structure. These materials are characterized by polarization properties that differ dramatically from those of the standard III-V compounds considered so far. From simple symmetry arguments,¹⁷ it can be shown that wurtzite semiconductors are characterized by a non-zero polarization in their equilibrium (unstrained) geometry, named spontaneous polarization (or, occasionally, pyroelectric, with reference to its change with temperature).¹⁸ While the spontaneous polarization of ferroelectrics can be measured via an hysteresis cycle, in a wurtzite this cannot be done, since no hysteresis can take place in that structure. Indeed, spontaneous polarization has never been measured directly in bulk wurtzites so far. III-V nitride MQWs offer the opportunity to reveal its existence and to actually measure it. In turn, spontaneous polarization can provide new degrees of freedom, in the form of permanent *strain-independent* built-in electrostatic fields, to tailor transport and optical characteristics of nitride nanostructures. Its presence can *e.g.* be exploited to cancel out the piezoelectric fields produced in typical strained nitride structures, as discussed below.

Thanks to recent advances¹⁹ in the modern theory of polarization (a unified approach based on the Berry's phase concept), it has become possible to compute easily and accurately from first principles the values of the spontaneous polarization, besides piezoelectric and dielectric constants, in III-V nitrides.^{1,2} The results of the calculations show that III-V nitrides have important polarization-related properties that set them apart from standard zincblende III-V semiconductors:

- i) huge piezoelectric constants (much larger than, and opposite in sign to those of all other III-V's);
- ii) existence of a spontaneous polarization of the same order of magnitude as in ferroelectrics.

The latter is, we think, a most relevant property. Spontaneous polarization implies that even in heterostructure

systems where active and cladding layers are both lattice-matched to the substrate (so that no strain occurs, hence no piezoelectricity), an electric field will nevertheless exist due to spontaneous polarization. In addition, unlike piezoelectric polarization, spontaneous polarization has a *fixed direction* in the crystal: in wurtzites it is the (0001) axis, which is (as mentioned previously) the growth direction of choice for nitrides epitaxy. Therefore the field resulting from spontaneous polarization will point along the growth direction, and this (a) maximizes spontaneous polarization effects in these systems, and (b) renders the problem effectively one-dimensional. In the simplest case of a fully unstrained (substrate lattice-matched) MQW, the electric fields inside the layers are given, in analogy to Eq. 2, by

$$\begin{aligned} \mathbf{E}_A^{(\text{sp})} &= 4\pi\ell_C(\mathbf{P}_C^{(\text{sp})} - \mathbf{P}_A^{(\text{sp})})/(\ell_C\epsilon_A + \ell_A\epsilon_C) \\ \mathbf{E}_C^{(\text{sp})} &= 4\pi\ell_A(\mathbf{P}_A^{(\text{sp})} - \mathbf{P}_C^{(\text{sp})})/(\ell_C\epsilon_A + \ell_A\epsilon_C) \end{aligned} \quad (5)$$

where the superscript (sp) stands for spontaneous; typical spontaneous polarization values¹ indicate that these fields are very large (up to several MV/cm).

In actual applications (for instance, to produce unstrained MQWs) alloys will have to be employed. The values of the spontaneous polarization are accurately known only for binary compounds.¹ In the absence of better estimates, we assume as before that the spontaneous polarization in alloys can be estimated using a Vegard-like rule as (for, *e.g.*, $\text{Al}_x\text{In}_y\text{Ga}_{1-x-y}\text{N}$)

$$\mathbf{P}^{(\text{sp})}(x, y) = x \mathbf{P}_{\text{AlN}}^{(\text{sp})} + y \mathbf{P}_{\text{InN}}^{(\text{sp})} + (1-x-y) \mathbf{P}_{\text{GaN}}^{(\text{sp})}.$$

In Figure 1 we report the resulting spontaneous polarization vs. lattice constant for the III-V nitrides, with data from Ref. 1.

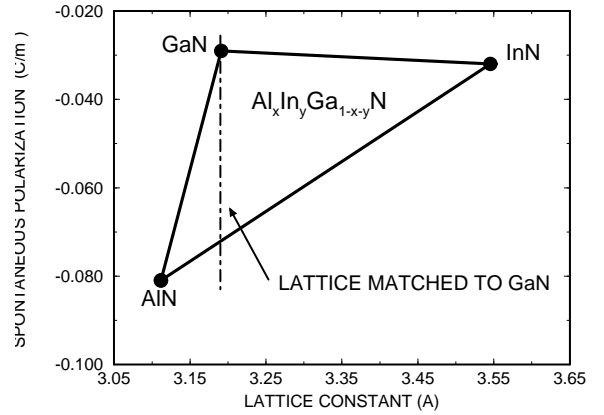


FIG. 1. Spontaneous polarization in $\text{Al}_x\text{In}_y\text{Ga}_{1-x-y}\text{N}$ alloys according to a Vegard-like rule.

Figure 1 shows that for a given (substrate) lattice constant, a wide interval of spontaneous polarizations (hence of spontaneous fields, according to Eq. 5) is accessible varying the alloy composition. In particular, consider a GaN/ $\text{Al}_x\text{In}_y\text{Ga}_{1-x-y}\text{N}$ MQW, where the composition

is chosen so that the alloy be lattice matched to GaN, which we assume to be also the substrate (or buffer) material (dashed-dotted line in Figure 1). Then, piezoelectric polarization vanishes, but spontaneous polarization remains, and takes on values up to ~ 0.05 C/m². For a GaN quantum well with thick AlGaIn cladding layers, this means a theoretical electrostatic field of up to about 5 MV/cm.

IV. FIELDS IN THE GENERAL CASE

In general, of course, MQWs will be strained. Then, for an arbitrary strain state, the electric fields in the A (or C) layers of the MQW are *the sum* of the piezoelectric and spontaneous contributions:

$$\mathbf{E}_{A,C} = \mathbf{E}_{A,C}^{(sp)} + \mathbf{E}_{A,C}^{(pz)},$$

where $\mathbf{E}^{(pz)}$ is the old-fashioned piezoelectric field from Eq. 2, and $\mathbf{E}^{(sp)}$ is given by Eq. 5. It is important to stress that $\mathbf{E}^{(sp)}$ depends only on material composition and not on the strain state. Also, it is a key point to notice that although both polarization contributions lay along the same direction [the (0001) axis], $\mathbf{P}^{(pz)}$ may have (due to its strain dependence) the same or the opposite sign with respect to the fixed $\mathbf{P}^{(sp)}$ depending on the epitaxial relations.

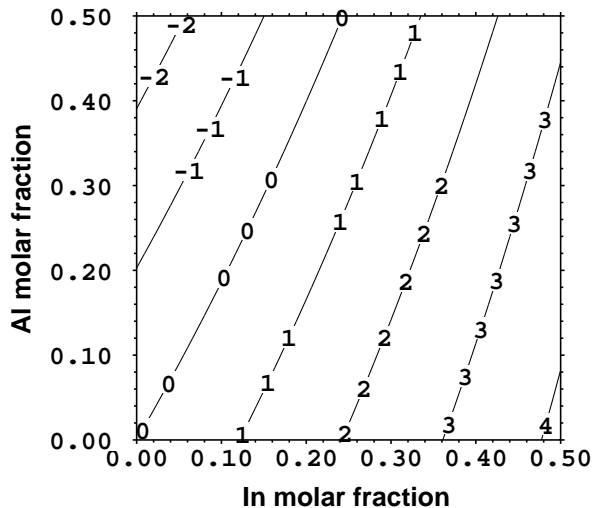


FIG. 2. Total built-in electrostatic field in the active layer of a $\text{Al}_x\text{In}_y\text{Ga}_{1-x-y}\text{N}/\text{GaN}$ MQW system (see text) vs. Al and In molar fraction. Fields are in units of MV/cm, positive fields point in the (0001) direction (Ga-face).

It is difficult to give a simple picture of the electric field pattern in a general MQW system because of the many degrees of freedom involved. Here we consider an $\text{Al}_x\text{Ga}_y\text{In}_{1-x-y}\text{N}/\text{GaN}$ MQW pseudomorphically grown over a GaN substrate, having active and cladding layers of the same thickness. In such a case

$$\mathbf{E}_A^{(sp)} + \mathbf{E}_A^{(pz)} \equiv \mathbf{E}_A = -\mathbf{E}_C \equiv -(\mathbf{E}_C^{(sp)} + \mathbf{E}_C^{(pz)}).$$

Note again, at this point, that the fields (see Eqs. 2 and 5) are not related to just the polarization of the material composing the specific layer, but a combination of polarization *differences*, dielectric screening, and geometrical factors.²⁰ We now consider the field values in the active layer: the total field \mathbf{E}_A is shown in Figure 2 vs. Al and In molar fraction; the same is done for the piezoelectric component in Figure 3. In both cases the appropriate Vegard-like rules have been used.

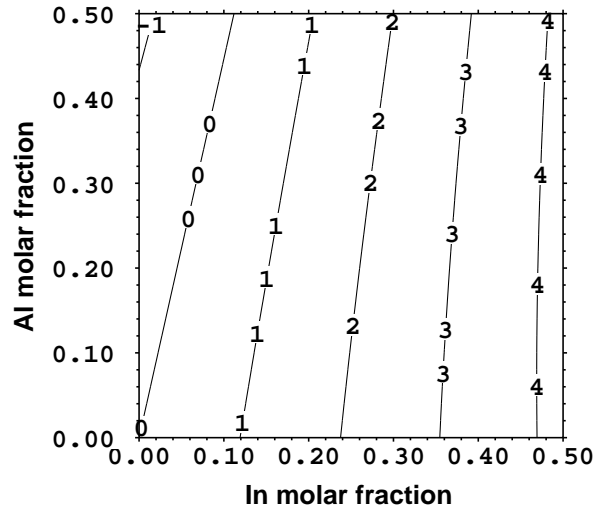


FIG. 3. Piezoelectric component of the electrostatic fields in the same MQW system as in Figure 2 (see text).

Comparison of these Figures clearly bears out the importance of spontaneous polarization in determining the electric field. Several aspects are worth pointing out. First, large electric fields (~ 0.5 – 1 MV/cm) can be obtained already for modest Al and In concentrations. Second, it is easy to access compositions such that $\text{Al}_x\text{In}_y\text{Ga}_{1-x-y}\text{N}$ is lattice matched to GaN: thereby, no piezoelectric fields exist, but large, purely spontaneous fields still do; specifically, this situation is realized for compositions laying on the zero-piezoelectric-field line in Figure 3. On this locus of compositions, spontaneous polarization is the only source of field and it can therefore be measured via the changes it induces in the MQW spectra. Third, it is possible to choose the material composition in such a way that the active layers of a MQWs are free of electric fields. To achieve this situation the MQW must be strained so that the piezoelectric and spontaneous polarizations cancel each other out; clearly, this is realized for compositions laying on the zero-field line in Figure 2. Of course the possibility of having a null field where desired is of capital importance in those devices where electric fields in the active layer can not be tolerated (other field screening mechanisms are discussed below).

A noticeable feature of Figure 3 is that the piezoelectric component increases much faster with In content than

with Al content, despite the larger piezoelectric constants of the latter. The reason is, of course, that strain builds up much more rapidly with In concentration. Along with the small difference in spontaneous polarization between InN and GaN, this is the reason why it is possible to interpret with reasonable accuracy polarization effects in InGa_xN/GaN structures on the basis of purely piezoelectric effects, as done in Refs. 9–11. On the other hand, it can be seen that the *spontaneous* component increases much more rapidly with Al content than with In content, due to the widely different polarizations of AlN and GaN. For AlGa_xN, piezoelectricity-based interpretations are bound to fail.

V. EFFECTS OF POLARIZATION FIELDS

We now come to the implications of polarization fields for devices based on III-V nitrides. In this Section we present a set of accurate self-consistent tight-binding calculations for an isolated AlGa_xN/GaN QW representing a system in which the the spontaneous-polarization contribution to the total built-in electrostatic field is as large as the piezoelectric term. To simulate realistically these nanostructures, self-consistency is needed to describe field screening by free carriers; the latter cannot physically cancel out the polarization charge, which is fixed and invariable, but may screen it out in part. In our calculations we therefore solve self-consistently the Poisson equation and the Schrödinger equation for a state-of-the-art empirical tight binding Hamiltonian for realistic nanostructures.²¹ In the following, two cases are considered: (a) non-equilibrium carrier distribution (Subsec. A and B) related to photoexcitation or injection, where electron and hole quasi-Fermi levels are calculated for a given areal charge density (n_{2D}) in the quantum well (the sheet density, related to the injection current or optical pumping power); (b) thermal equilibrium distribution (Subsec. C and D) where the Fermi level is calculated as a function of doping density by imposing charge neutrality conditions.²¹ We solve Poisson's equation,

$$\frac{d}{dz}D = \frac{d}{dz} \left(-\varepsilon \frac{d}{dz}V + P_T \right) = e(p - n), \quad (6)$$

where the (position-dependent) quantities D , ε , and V , are respectively the displacement field, dielectric constant, and potential. P_T is the (position-dependent) total transverse polarization. The effects of composition, polarization, and free carrier screening are thus included in full. [Consistently with the aim of describing a *single* QW, we choose boundary conditions of zero field at the ends of the simulation region. This corresponds to the $\ell_C \rightarrow \infty$ limit in Eqs. 2 and 5.]

The potential thus obtained is inserted in the Schrödinger equation, which is solved diagonalizing an empirical tight-binding $sp^3d^5s^*$ Hamiltonian.²² The procedure is iterated to self-consistency. Further appli-

cations and details on the technique can be found elsewhere.^{7,21}

Here we concentrate in particular on the polarization-induced quantum-confined Stark effect (QCSE) in zero external field, its control and quenching, and its evolution with layer thickness. We first deal with the low free-carrier densities regime: thereby the QCSE manifests itself as a strong red shift of the interband transition energy, with a concurrent suppression of the transition probability, both of these features getting stronger as the well thickness increases. This is the regime that applies to low-power operation or photoluminescence experiments.

Next we discuss how the QCSE can be modified, and eventually (almost) quenched, by providing the QW with a sufficiently high free-carrier density. In this regime, as the free carrier density increases, the transition energy is progressively blue-shifted back towards its flat band value, and the transition probability suppression is largely removed. The needed free-carrier density depends on the polarization field, and not surprisingly it is found to be very substantial. Typical values of the sheet density range in the 10^{13} cm^{-2} , as opposed to typical values of 10^{12} cm^{-2} needed to obtain lasing in GaAs-like materials.

A. QCSE at low power

The prototypical system we consider is an isolated GaN quantum well cladded between Al_xGa_{1-x}N barriers. In Figure 4, we display the total field \mathbf{E}_A in the (isolated) active well, and its piezoelectric component as a function of the Al molar fraction x . The spontaneous component is the difference of the two, and therefore approximately equal to the piezoelectric one.²³

The value we pick for our simulations is $x=0.2$, a reasonable compromise between the conflicting needs for not-too-large fields, sufficient confinement, and technologically achievable composition. In this case the valence offset is $\Delta E_v = 0.064 \text{ eV}$. The total field in the QW of -2.26 MV/cm , and the spontaneous and piezoelectric components are -1.14 MV/cm and -1.12 MV/cm respectively. The minus signs indicates that the field points in the $(000\bar{1})$ direction. The bare polarization charge at the interface is proportional to the change in polarization across the interfaces, and it amounts to $\sim 1.28 \times 10^{13} \text{ cm}^{-2}$. The *field* value mentioned above results from this charge as screened by the dielectric response of the QW (the field change at the interface is thus related to a smaller, or screened, effective interface charge³).

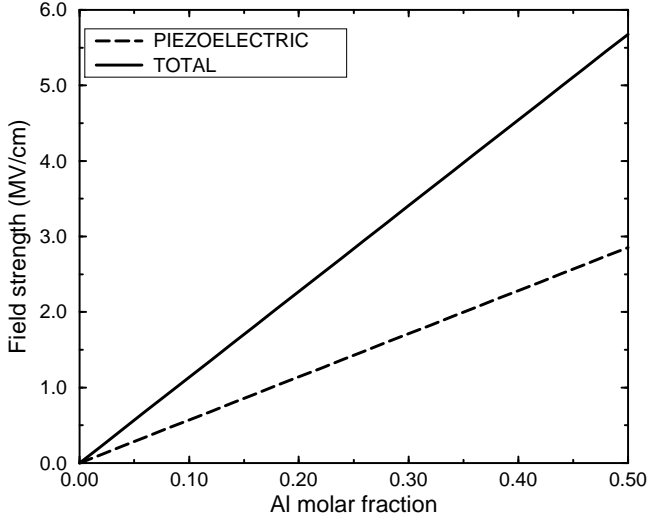


FIG. 4. Total field and its piezoelectric component in the GaN/Al_xGa_{1-x}N QW discussed in the text.

We performed a series of calculations for different well widths, where the electron and hole confined states have been populated (*i.e.* pairs have been created) with a density of $\sim 10^{11} \text{ cm}^{-2}$ to simulate a low-power optical excitation. We find that this density has only a very marginal effect: indeed, the potential is perfectly linear, *i.e.* the electrostatic field remains uniform, over the whole QW. The square-to-triangular change in the potential shape causes a small blue shift of both the electron and hole confined states (referred to the flat well bottom), but the linear potential given by the field causes a much larger relative red shift for any reasonable thickness. Also, since the thermal carrier density fluctuations are negligible at microscopic thicknesses and room temperature (see below, and Ref. 24), one expects the QW band edge profile to remain linear as a function of thickness, at least for the low excitation powers typical of photoluminescence spectroscopy.

In Figure 5 we show the TB result for the lowest interband transition energy and the corresponding transition probability (*i.e.* the squared overlap of the highest hole level and the lowest electron level envelope wavefunctions²¹) as a function of QW thickness. Both the Stark red shift and the strong suppression of the transition probability are evident. This was to be expected from the potential shape and the reduced overlap of hole and electron states, displayed in the inset of Figure 5.

It is worth noting that the localization of the hole envelope function in the well region is rather weak, because the large effective field blue-shifts the hole bound state energy close to the valence barrier edge. This will generally be the case for low- x AlGa_N wells, due to the small valence confinement energy.³ Indeed, even the conduction confinement is small on the scale of the fields-induced potential drop, and the electron bound state also tends to

have the character of a resonance for small x (*i.e.* small confinement).

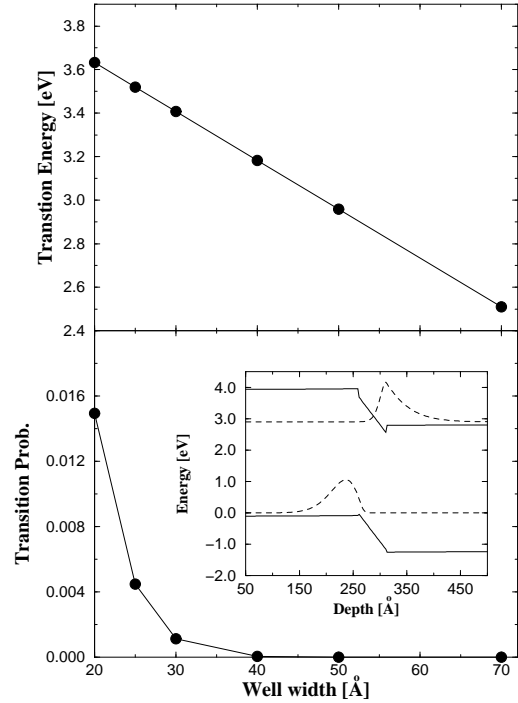


FIG. 5. Transition energy red shift and suppression of transition probability vs well thickness. In the inset self-consistent band edge (solid), electron and hole envelope functions of the TB wavefunctions (dashed) for a 50 Å thick QW.

We conclude that in the absence of excitation and at normal operation temperatures, or at low optical excitation power, macroscopic polarization fields cause QW's to be highly inefficient in emitting light, and the emission energy to be considerably different than the gap of the material plus the confinement energies.

Comparison with experiment is tricky since most attempts to measure these effects are polluted by inappropriate (at least for the purpose of revealing polarization effects) choices of the experimental geometry. For instance, measurements have been done⁴ in a *series* of quantum wells of different thicknesses ranging between 10 and 50 Å.²⁵ In any case, the general experimental features^{4,10,9,26} are in full agreement with the notion that the transitions are red-shifted essentially linearly with increasing well thickness, and that screening at low free carrier densities is irrelevant in this class of systems. This is not quite true any more for thick layers, as will be discussed in Sec.V C.

B. QCSE quenching at high excitation power

If carriers are generated optically, one can envisage that a sufficiently high excitation power could possibly produce the carrier density needed to screen the polarization field. We now calculate the properties of the QW as a function of the free-carrier areal density, to check if the red shift and the transition probability suppression can be removed in a physically accessible range of such density.

We repeat the self-consistent procedure increasing progressively the free charge density in the QW from 10^{12} up to $2 \times 10^{13} \text{ cm}^{-2}$. We see in Figure 6 that, albeit at the cost of a large increase of the QW free-carrier density, the field does get progressively screened.

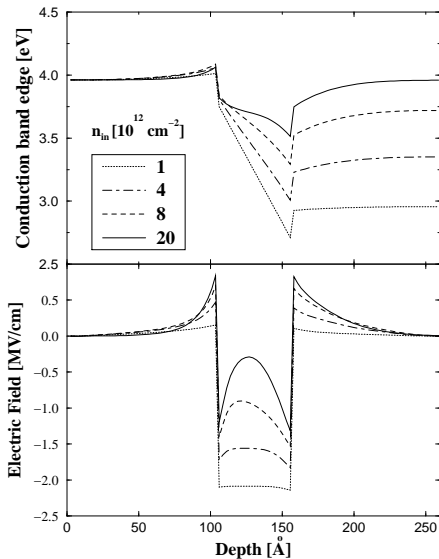


FIG. 6. Self-consistent band edge (a) and electric field (b) for various sheet densities (\sim excitation level) in a 50 Å thick QW.

As can be seen in Figure 7, at fixed thickness the red shift decreases as the carrier density increases, and it tends to become thickness-independent at the highest densities. The transition probability is also increased by several orders of magnitude. However, the field is not screened abruptly but dies off gradually, with an effective screening length of about 20 Å for the largest density used here (of course, this is a token of the larger spatial extension of the screening charge as compared to the polarization charge³): hence, holes and electron remain spatially separated to a large extent even at high carrier densities, and the transition probability never quite goes back to unity. This is likely to be one of the reasons for the relatively low quantum efficiency observed in typical nitride MQW devices. For the same reasons, the transi-

tion energy never quite goes back to the flat-band value (gap plus confinement energy). Note in passing that because of strain, in these calculations $E_g^{\text{GaN}} = 3.71 \text{ eV}$, almost 10 % larger than the equilibrium value.

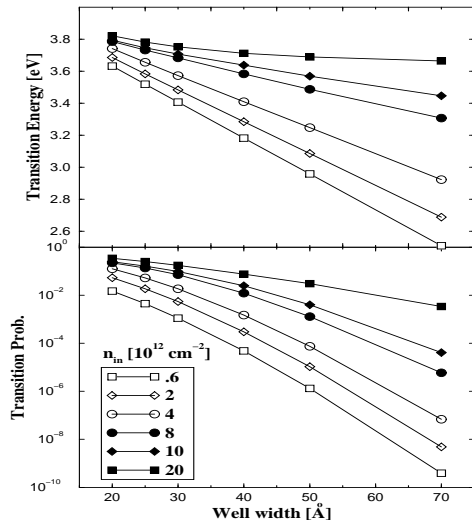


FIG. 7. Removal of red shift and recovery of interband transition probability upon high excitation.

The screening density of order $2 \times 10^{13} \text{ cm}^{-2}$ needed to partially screen out the field corresponds to an estimated²⁷ optical pumping power of about 10 to 20 kW/cm^2 per well. This figure agrees nicely with the unusually high pumping powers^{4,10,26,28} needed to obtain the laser effect in nitride structures. The explanation is simply that much of the free charge being generated actually goes into screening the polarization field. On the other hand, our result prove that the optically activated lasing conditions can indeed be realized in practice, although with high pumping powers, so that there seems to be no need to invoke quantum dot formation²⁰ or other exotic effects to explain lasing in nitride structures. On the other hand, the same phenomenon explains the high current threshold observed for electrically driven GaN based lasers.^{29–31}

QCSE quenching phenomena similar to those just described have been observed⁹ by Takeuchi *et al.* in In-GaN/GaN MQWs, with estimated fields in the 1 MV/cm range. The red shift and optical inefficiency were in fact removed, although only in part and in a transient fashion, by sufficiently high excitation powers. The order of magnitude of the values reported in Ref. 9 is $\sim 200 \text{ kW/cm}^2$ for 5 to 10 MQW periods, *i.e.* 20 to 40 kW/cm^2 per well, in qualitative agreement with our estimate above.

One important remark at this point is that, depending on the excitation power, the MQW will adsorb radiation at many different transition energies ranging from that of the built-in-field-biased well (low power limit) to the quasi-flat-band well (high power limit) – that is, the

MQW acts a multistable switch. It is indeed fortunate that the typical fields in these structures are such that one can physically access the various possible regimes.

Another noticeable effect is that at a properly chosen value of the sheet density (*i.e.* of the excitation power) one can obtain at the same time a reasonable transition probability *and* a red-shifted energy by just increasing the well thickness. This is very useful since the transition wavelength can be shifted to a different color without changing alloy composition, but only the well thickness. For instance (see Figure 7), changing the well thickness from 20 to 30 Å at a sheet density of $4 \times 10^{12} \text{ cm}^{-2}$, one obtains an energy red shift of 0.1 eV at the cost of a loss of a factor 10 in recombination rate, which may still be acceptable depending on the application. Red-shifting the transition energy in this fashion may avoid the need to add *e.g.* some In in the QW composition. Of course, *blue*-shifting by thickness reduction will increase the transition probability.

C. Self-screening of fields in massive samples

Free charge produced by high excitation screens polarization fields fairly efficiently over the quite short distances typical in nanostructures, basically because the spatial extension of the screening charge is comparable to the size of the system. How about extended samples, especially if not subjected to illumination, *i.e.* having only intrinsic free carriers? It is indeed the case that no macroscopic fields exist in “infinitely large” samples even in the absence of high densities of (say) photogenerated carriers. The simple reason is that the intrinsic carrier fluctuations in an undoped semiconductor rise exponentially as a function of deviations of the chemical potential from the mid-gap value.²⁴ In polarized nitrides, such deviations occur due to the built-in fields. As the sample thickness increases, the potential drop grows linearly. When the drop is smaller than the gap, the field is uniform: $|\mathbf{E}| = 4\pi\mathbf{P}/\epsilon_0$. When the drop approaches the gap value, *i.e.* for thicknesses approaching $d_c = E_{\text{gap}}/|\mathbf{E}|$, the Fermi level nears the band edges: consequently, large amounts of holes and electrons are generated on the opposite sides of the sample. These intrinsic carriers screen partially the polarization charges, preventing the gap from closing. The total potential drop is thus pinned at the gap value for all thicknesses $d > d_c$ – that is, the effective gap decreases down to zero, but not below. For $d > d_c$, the field will decrease as

$$|\mathbf{E}| = E_{\text{gap}}/d.$$

For this picture to hold, the spatial extension of the screening charge at the sample surface must be comparable with that of the polarization charge (a few Å at most³) and much smaller than the sample size. This will cause the field inside the sample to remain uniform, since the net effect of screening will be to change the effective

polarization charge. Indeed, this assumption turns out to be verified in practice on direct inspection, as we discuss below.

Clearly, the above mechanism will strongly influence QW’s of thicknesses equal to, or larger than, the critical value d_c . For the system we are considering here, with a built-in field of -2.26 MV/cm , the critical value is $d_c \sim 165 \text{ Å}$. To confirm our picture, we simulated QW’s with the same composition and geometry considered in Subsec. B, and thicknesses below and above d_c , to mimic the crossover from a “microscopic” to a “macroscopic” sample. In this case, we need to describe very extended bulk regions on the left and right of the QW, in order to account for the large screening length. Thus, we have made use of a classical Thomas-Fermi model, where the charge densities are calculated with Fermi-Dirac statistics of a classical system rather than by solving the Schrödinger equation in the TB basis. This allows to consider devices with a spatial extension of several hundreds of microns. Effective masses in this calculation were fitted to accurately reproduce the self-consistent TB results.

The resulting self-consistent potential is shown in Figure 8 for well thicknesses of 100, 200, 300, and 400 Å. A first point to note is that the field remains uniform for all well thicknesses. The field value equals the polarization field for the smallest thickness (smaller than d_c); for the thicker wells, the field (while remaining uniform) indeed decreases progressively as $\propto 1/d$.

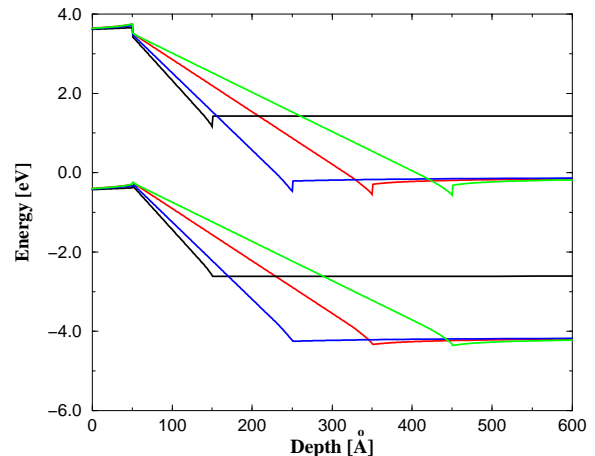


FIG. 8. Field self-screening in a thick layer near and above the critical thickness.

Photoluminescence experiments are not expected to be able to reveal this effect (which should cause a saturation of the red shift as function of thickness) in very thick QW’s, since the effective recombination rate rapidly becomes vanishingly small. Experiments aiming to reveal this effect should be designed considering our result, that a very thick layer is effectively subjected to a uniform electrostatic field E_{gap}/d . In an unstrained GaN QW,

for $d > d_c$ (the latter being typically of order 100-200 Å or so depending on the polarization) the field is $\sim 3.4 \text{ V}/d$, *i.e.* $\sim 70 \text{ kV}/\text{cm}$ for $d = 0.5 \mu\text{m}$. This is presumably sufficient to cause observable bulk-like effects such as shifts in response functions or field effects on impurities.

A similar “self-screening” behavior has been revealed indirectly in devices comprising sufficiently thick layers. In Ref. 32 a 300 Å thick $\text{Al}_{0.15}\text{Ga}_{0.85}\text{N}$ layer was grown on a very thick GaN substrate, and topped with a Schottky contact. The predicted field in the AlGaN layer is 1.4 MV/cm, which would cause a potential drop of 4.2 eV across the layer. The maximum reasonable potential drop dictated by Schottky barriers, conduction offset, and Fermi level is about 1 eV, so it must be the case that the polarization charge gets largely screened by electrons from the GaN layer, forming a high-density two-dimensional electron gas (2DEG) at the heterointerface; this, by the way, causes an enhanced conductivity in the active channel. CV depth profiling indeed reveals a 2DEG at the interface.³² An equivalent, more formal description is that the field would force the metal-determined Fermi level to some 3 eV above the conduction band of GaN, thus attracting towards the interface an enormous carrier density, which screen out (part of) the field. Note in passing that in Ref. 32 only piezoelectric polarization was considered, which leads to an underestimation of the 2DEG density, since the piezoelectric contribution is actually about one third of the total interface charge. Similar considerations apply to other similar experiments.³³ The recent device simulation of Ref. 8 has corrected this point, including in part the spontaneous-polarization interface charges.

D. Suppressing QCSE by doping

We have seen in the previous Sections that polarization fields can be screened to a reasonable extent by generation of free charge of *both* kinds in the QW upon *e.g.* optical excitation. Qualitative problems with this screening mechanism are that (a) it is transient, since it disappears when photoexcitation or current injection are removed, and that (b) in purely electronic (*i.e.* non-optoelectronic) devices, it is unlikely that the high densities needed can be reached in normal operating conditions. Besides, the current is not constant in time, so that the well shape also changes in time.

It is natural to presume that the same effects can be achieved in a permanent fashion using extrinsic carriers from dopants. The idea is to provide the well with carriers which would screen the polarization charge, excepts that now the electrons are released into the QW from the doped barriers, and not injected or photogenerated. Of course, this effect is not transient as the others discussed previously. The problem is, how high must the doping density be to achieve the same level of screening as in a high optical excitation regime. We simulated a 50

Å thick $\text{Al}_{0.2}\text{Ga}_{0.8}\text{N}/\text{GaN}$ single QW, where the barriers have been doped *n*-type in the range from 10^{17} to 10^{20} cm^{-3} and the donor ionization energy³⁴ have been set to 10 meV. In this simulation, we used again the self-consistent TB approach. The resulting conduction band profile is displayed in Figure 9 for the various doping densities.

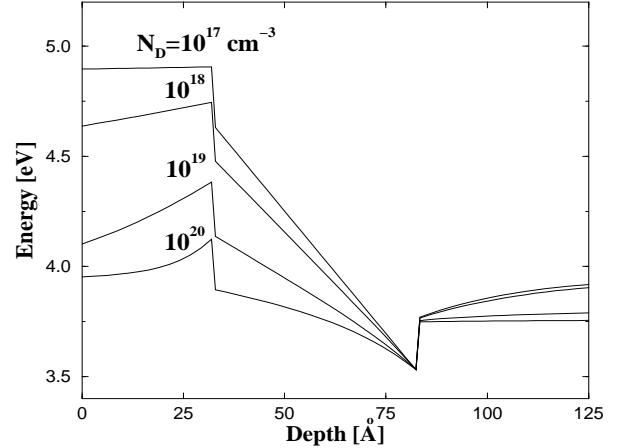


FIG. 9. Conduction band edge of a remotely-doped GaN/AlGaN quantum well.

The polarization field raises the conduction band on the left side over the Fermi energy, and in order for the barrier conduction band to reach the Fermi level on the far left, the electrons are transferred from the left-side barrier into the QW, leaving behind a large depletion layer. As a consequence of the electron flow into the QW, the polarization field starts to get significantly screened at doping densities above $\sim 10^{19} \text{ cm}^{-3}$. The existence of a depletion layer causes a large band bending in the left-side barrier, while the bending is absent in the left half of the well. This is quite different to the case of the photoexcited well, where the bending on the left side of the well was due to hole accumulation near the interface (see Figure 6). This explains why the field remains nearly uniform in the left half of the well for all of the simulations performed. On the right side of the well, only a small bending due to the electron accumulation is present. Indeed electron localization is quite weak in these systems, since the confinement potential is small as compared to the field-induced drop, and electrons tend to spill over to the right-side barrier. This is likely to be the case in all nitride systems in this composition range.

From these results, we conclude that doping can indeed be used to screen polarization fields. While it is not obvious that the needed doping level can always be reached in practice, it is likely that a combination of doping and current injection or photoexcitation will generally succeed in quenching polarization fields in the range of MV/cm, thus allowing for recovery of quasi flat band conditions. Fields in InGaN/GaN systems will be generally smaller

than those in AlGaIn/GaN systems for typical compositions in use today, and will therefore be more easily amenable to treatment by the above technique. This procedure has in fact been adopted in experiment by Nakamura's group,¹⁰ which reported that a doping level of 10^{19} cm^{-3} is sufficient to quench the QCSE to a large extent. Indeed, in their $\text{In}_{0.15}\text{Ga}_{0.85}\text{N}/\text{GaN}$ MQWs the unscreened field is $\sim 1.2 \text{ MV/cm}$, *i.e.* approximately a half of the one we considered here. This field will be more easily screened by remote doping, in qualitative agreement with our findings.

VI. SUMMARY AND ACKNOWLEDGEMENTS

In conclusion, we have discussed how macroscopic (and in particular, spontaneous) polarization plays an important role in nitride-based MQWs by producing large built-in electric fields. Contrary to zincblende semiconductors, in III-V nitrides-based devices the spontaneous polarization is an unavoidable source of large electric fields even in lattice-matched (unstrained) systems. The existence of these fields may also be used as additional degree of freedom in device design: for instance, for an appropriate choice of alloy composition, spontaneous and piezoelectric fields may be caused to cancel out, thus freeing the structures from built-in fields. We have also discussed the different regimes of free carrier screening, effected by doping or optical excitation, showing that fields can be screened only in the presence of high free carrier densities, which leads to unusually high lasing thresholds for undoped QW's. Of course, our results about the effects on the electronic structure apply qualitatively to any kind of polarization field, thus in particular also to piezo-generated ones.

VF and FB acknowledge special support from the PAISS program of INFN. VF's stay at the Walter Schottky Institut was supported by the Alexander von Humboldt-Stiftung. FDS, ADC and PL acknowledge support from Network Ultrafast and 40% MURST.

¹ F. Bernardini, V. Fiorentini, and D. Vanderbilt, Phys. Rev. B **56**, R10024 (1997).

² F. Bernardini, V. Fiorentini, and D. Vanderbilt, Phys. Rev. Lett. **79**, 3958 (1997); F. Bernardini and V. Fiorentini, Phys. Rev. B **58** 15292 (1998).

³ F. Bernardini and V. Fiorentini, Phys. Rev. B **57**, R9427 (1998).

⁴ M. Leroux, N. Grandjean, M. Laißt, J. Massies, B. Gil, P. Lefebvre, and P. Bigenwald, Phys. Rev. B **58**, 13371 (1999).

⁵ R. Cingolani, M. Lomascolo, G. Coli, F. Della Sala, A. Di Carlo, and P. Lugli, to be published.

⁶ M. Buongiorno Nardelli, K. Rapcewicz, and J. Bernholc, Appl. Phys. Lett. **71**, 3135 (1997).

⁷ F. Della Sala, A. Di Carlo, P. Lugli, F. Bernardini, V. Fiorentini, R. Scholz, and J.-M. Jancu, Appl. Phys. Lett. **74**, 2002 (1999).

⁸ R. Oberhuber, G. Zandler, and P. Vogl, Appl. Phys. Lett. **73**, 818 (1998).

⁹ T. Takeuchi, S. Sota, M. Katsuragawa, M. Komori, H. Takeuchi, H. Amano and I. Akasaki, Jpn. J. Appl. Phys. **36**, L382.

¹⁰ T. Deguchi, A. Shikanai, K. Torii, T. Sota, S. Chichibu, and S. Nakamura, Appl. Phys. Lett. **72**, 3329 (1998); S. Chichibu *et al.*, Appl. Phys. Lett. **73**, 2006 (1998).

¹¹ L.-H. Peng, C.-W. Huang, and L.-H. Lou, Appl. Phys. Lett. **74**, 795 (1999);

¹² S.-H. Park and S.-L. Chuang, Phys. Rev. B **59**, 4725 (1999) and references therein.

¹³ From dielectric displacement conservation (see Ref. 2) one gets $4\pi(P_C - P_A) = \epsilon_A E_A - \epsilon_C E_C$. Periodicity implies $\ell_A E_A + \ell_C E_C = 0$. Solving for one of the fields, Eqs.2 are immediately obtained.

¹⁴ This assumption is valid in the limit in which the electric field across the whole structure is negligible with respect to the internal fields induced by polarization.

¹⁵ Note that for normal devices layered along the nominal growth direction, the electric field is always parallel to the growth direction, even if the polarization is not.

¹⁶ Vegard-like estimates of the polarization should of course be considered with caution, as it is established (see *e.g.* P. Ernst, C. Geng, M. Burkard, F. Scholz, and H. Schweizer, in *The Physics of Semiconductors*, M. Scheffler and R. Zimmermann eds. (World Scientific, 1996), p. 469; S. Froyen, A. Zunger, and A. Mascarenhas, Appl. Phys. Lett. **68**, 2852 (1996)) that ordering in (cubic) III-V solid solutions can produce spontaneous polarization, an effect not unexpected also in the XN's. Even in the random solution, short-range order in the form of bond alternation may alter the local electronic structure, hence the polarization. We are currently investigating this problem.

¹⁷ J. F. Nye, *Physical properties of crystals* (Oxford UP, 1985).

¹⁸ One possible way to see it is as the zero-strain limit of the piezoelectric polarization.

¹⁹ R. D. King-Smith and D. Vanderbilt, Phys. Rev. B **47**, 1651 (1992). R. Resta, Rev. Mod. Phys. **66**, 899 (1994).

²⁰ This contradicts some of the assumptions and conclusions of Ref. 6.

²¹ A. Di Carlo *et al.*, Solid State Communications **98**, 803 (1996); A. Di Carlo, MRS Proc. **491** 389 (1998).

²² J.-M. Jancu, R. Scholz, F. Beltram, and F. Bassani, Phys. Rev. B **57**, 6493 (1998);

²³ Since we use the *calculated* lattice constants of III-V nitrides to determine strains, the piezoelectric component may be overestimated due to the slight underestimation of a_{AlN} .

²⁴ N. W. Ashcroft and N. D. Mermin, *Solid State Physics*, (Holt-Saunders Japan, Tokio 1981), p.576 and p.611.

²⁵ In Ref. 4 the red shift was found to be compatible with a field of 450 kV/cm, to be compared with the predicted values of piezoelectric field, 120 kV/cm, and total field, 640 kV/cm. The obvious source of uncertainty in the polar-

ization values extracted from this experiment are of course the intricate and not uniquely defined boundary conditions produced by the awkward choice of geometry. We note further that the agreement with the total field would improve in the case of epitaxial relaxation.

- ²⁶ J. S. Im, H. Kollmer, J. Off, A. Sohmer, F. Scholz, and A. Hangleiter, Phys. Rev. B **57**, R9435 (1997).
- ²⁷ A. Niwa, T. Ohtoshi, and T. Kuroda, Jpn. J. Appl. Phys., **36**, L771 (1997); I. Nomura, K. Kishino, A. Kikuchi, Solid-State Electron. **41**, 283 (1997); R. J. Radtke, U. Waghmare, H. Ehrenreich, and C. H. Grein, App. Phys. Lett. **73**, 2087 (1998)
- ²⁸ K. Domen, A. Kuramata, and T. Tanahashi, App. Phys. Lett., **72**, 1359 (1998).
- ²⁹ S Nakamura *et al.*, App. Phys. Lett. **72**, 2014 (1998); *ibid.* **73**, 832 (1998).
- ³⁰ W. Fang, and S. L. Chuang, App. Phys. Lett. **67**, 751 (1995).
- ³¹ Y. C. Yeo, T. C.Chong, M. F. Li, and W.J. Fan, J. App. Phys. **84**, 1813 (1998).
- ³² E. T. Yu, G. J. Sullivan, P.M. Asbeck, C. D. Wang, D. Quiao, and S. S. Lau, Appl. Phys. Lett. **71**, 2794 (1997).
- ³³ R. Gaska, J.W. Yang, A.D. Bykhovski, M.S. Shur, V.V. Kaminskii and S. Soloviov, Appl. Phys. Lett. **71**, 3817 (1997).
- ³⁴ Doping of $\text{Al}_x\text{Ga}_{1-x}\text{N}$ becomes rapidly inefficient above $x\sim 0.45$ (see *e.g.* A. Fara, F. Bernardini, and V. Fiorentini, J. Appl. Phys. **85**, 2001 (1999), and references therein), but it is viable at the low x of interest here.